Applied Catalysis A: General 494 (2015) 48–56

Contents lists available at ScienceDirect

Applied Catalysis A: General

journal homepage: www.elsevier.com/locate/apcata

Isocyanate (NCO) evidence in the CO + NO reaction over palladium

Graciela R. Garda, Norberto J. Castellani *

Grupo de Materiales y Sistemas Catalíticos, IFISUR, Departamento de Física, Universidad Nacional del Sur, Av. Alem 1253, 8000 Bahía Blanca, Argentina

ARTICLE INFO

Article history:
Received 31 October 2014
Received in revised form 7 January 2015
Accepted 16 January 2015
Available online 25 January 2015

Keywords:
Isocyanate formation
Palladium catalyst
Chemisorption
NO + CO
DFT

ABSTRACT

In the present work the NCO formation from N and CO species is theoretically studied using a computational method based on density functional theory (DFT) and a periodic slab model. For that purpose, the (100) and (111) faces of Pd have been considered, with two different pathways on both surfaces comprising the displacement of CO species. The overall processes are endothermic on Pd(100) and exothermic on Pd(111) and the corresponding energy barriers are larger on Pd(100), compared to Pd(111). Hence, in agreement with the experimental data the NCO formation is more favored on Pd(111). The results are rationalized taking into account charge distributions and electronic structure parameters.

1. Introduction

The increasing requirements on automobile emission in the last decades urged an intense scientific interest to improve catalytic conversion technologies. The concerned contaminant gases are mainly nitrogen oxides, carbon monoxide and unburned hydrocarbons. A suitable way to eliminate them in the catalytic converters is by the simultaneous reduction of NO_x and oxidation of CO in order to obtain the harmless N_2, N_2O and CO_2 gases. The earlier catalyst formulations produced for this purpose consisted of particles composed by precious metals like Rh and Pt supported on SiO_2 and Al_2O_3, and later on, catalysts based on Pd were introduced, being the latter the most used alternative nowadays. For this reason, the CO + NO reaction has been widely studied both theoretically [1,2] and experimentally [3–8] on Pd-based catalysts. Particularly, the formation of NCO was predicted theoretically [9] on Pd surfaces and, in a series of works, the isocyanate (NCO) species was detected on catalysts containing Pd [3,5,10–12] if CO and NO are simultaneously present at about 500–650 K and under high pressures (~1–10^3 Torr). Goodman et al. investigated this specific aspect of the CO + NO reaction on well defined Pd surfaces using polarization modulation infrared reflection absorption spectroscopy (PM-IRAS) [3,13], observing the formation of NCO species only on Pd(111) at high pressure conditions, relevant for real catalysts. This species appears in the PM-IRAS spectra at 500 K and is extremely stable in the 300–650 K temperature range. As the presence of NCO species implies the NO dissociation, according to

$$NO_{ads} \rightarrow N_{ads} + O_{ads} \quad (1)$$

$$N_{ads} + CO_{ads} \rightarrow NCO_{ads}, \quad (2)$$

the NCO species can be used therefore as a sensitive sensor of the NO dissociation process, a crucial step in the CO + NO reaction. While the non pollutant gases will be obtained from the combination of adsorbed N, NO, O and CO species, the NCO radical would play the role of a spectator in the CO + NO reaction.

Otherwise, the experimental study of NCO adsorption on different metal surfaces was usually implemented through the adsorption of isocyanic acid (HNCO). In this process, the H–N bond of HNCO is broken and the NCO species becomes adsorbed. The latter can be characterized by the technique of reflection absorption infrared spectroscopy (RAIRS) [14–16].

Inspired by the experimental finding reported by Goodman's group, our interest is to provide a theoretical insight at the molecular level into the behavior of reacting species involved in the formation of NCO, and corroborate its presence on Pd(111) and not on Pd(100). At present, several theoretical works about CO and NO adsorption on (100) and (111) faces of Pd [1,2,9,17–26] are available but only a few reports about NCO adsorption on silver [27] and copper [28] clusters, on Ni(100), Cu(100) and Pd(100) surfaces [29–33]. A first principle study of NCO formation on the Cu_2O(111) surface [34] and a semiempirical molecular orbital calculation on the Pd(111) surface [9] were performed, but to the best of our knowledge no other first principle studies about NCO formation on Pd(111) have ever been reported.

* Corresponding author. Tel.: +54 291 4595141; fax: +54 291 4595142.
E-mail address: castella@criba.edu.ar (N.J. Castellani).

http://dx.doi.org/10.1016/j.apcata.2015.01.025
0926-860X/

In the present work, the NCO formation according to equation (2) is theoretically studied using a computational method based on density functional theory (DFT) with a periodic slab model. For that purpose, the (100) and (111) faces of Pd have been considered, which are the mostly exhibited by supported palladium particles [35–38].

2. Model and computational details

Our calculations were performed within the density functional theory (DFT) by using the Vienna Ab-initio Simulation Package (VASP) [39–41]. In this package, the Kohn–Sham equations are solved using a plane wave basis set; for that, good convergence was achieved with a cut-off energy of 400 eV for the kinetic energy. The projector augmented wave (PAW) method was used to describe the effect of the core electrons on the valence states [42,43]. The latter is a frozen core method which considers the exact shape of the valence wave functions instead of pseudo-wave functions. The exchange and correlation effects were calculated using the GGA functionals as expressed by Perdew and Wang (PW91) [44,45].

The Pd(100) and Pd(111) surfaces were represented by a periodic four-layers Pd slab. The adlayer was located on one side of the slab configuring (2×2) superstructures with a coverage of 1/4ML, that agrees with a high temperature reaction [1]. A three dimensional periodic cell was constructed by including a vacuum gap of ~14 Å in the perpendicular direction to the metallic surface. The thickness of this vacuum region was found to be adequate to eliminate any interaction between adsorbed molecules on adjacent metal slabs.

The two-dimensional Brillouin integrations were performed on a grid of $6 \times 6 \times 1$ Monkhorst–Pack special k-points, for Pd(100), and $5 \times 5 \times 1$, for Pd(111) [46]. The Methfessel–Paxton smearing with a width $\sigma = 0.2$ eV was applied and the reported total energies were extrapolated to $\sigma = 0$ eV [47]. All calculations were performed at the spin polarized level. The geometry of adsorbed species was allowed to relax completely together with the Pd atom positions of the two uppermost layers of the surface; the other two layers of metallic slab were fixed at the bulk geometry. The Pd–Pd interatomic distance for the bulk, optimized in a previous work [33], was 2.800 Å. To obtain the gas-phase CO and NCO energies, a large box of $20 \times 20 \times 20$ Å^3 size was used. In all cases, optimized geometries were achieved when forces on atoms were smaller that 0.01 eV/Å.

The adsorption energy (E_{ads}) was calculated as the difference between the energy of the adsorbed species ($E_{sp/Me}$) and the sum of the energies for the free surface (E_{Me}) and the gas-phase species (E_{sp}), accordingly to the following equation:

$$E_{ads} = E_{sp/Me} - E_{Me} - E_{sp} \quad (3)$$

A negative value indicates an exothermic chemisorption process.

Vibrational frequencies were calculated considering a harmonic approach for the potential energy minima. The corresponding Hessian dynamical matrix was calculated by a finite difference method where the atoms in the adsorbed molecule were independently displaced by ±0.005 Å along each cartesian coordinate direction. It was verified that E_{ads} minima are absolute by checking that all the dynamical matrix eigenvalues had real values. The nudged elastic band (NEB) method, implemented for VASP [48–50], was used in order to find the transition states and the energy barriers in the proposed reaction pathways. For that purpose, four images were applied and, if necessary, the energy profile was reevaluated in the proximity of the transition state by including new images until a single imaginary eigenvalue of ~400 cm^{-1} was obtained.

The electronic charge distribution of the NCO/Pd systems was analyzed by calculating the Voronoi charge of each atom [51]. Furthermore, the electronic structure for these systems and the interaction between the adsorbed species and substrate were analyzed by calculating the partial local density of states (pLDOS) for the atomic orbitals.

3. Results and discussion

3.1. CO, N and NCO adsorption

As a preliminary step in the study of the NCO formation, we considered the adsorption of different molecules involved in the N + CO → NCO process; each of them looked as an individual species. The corresponding E_{ads} values and geometrical parameters are summarized in Table 1, and compared with the available experimental and theoretical data. Taking into account that the CO dissociation barriers on Pd(100) and Pd(111) as reported by Hammer et al. are very high (4.1 eV and 4.4 eV, respectively) in contrast to those of NO (2.3 eV and 2.7 eV, respectively) [1], in this work the CO molecule will be considered a non-dissociated species, whereas the NO molecule will be treated as dissociated, providing the N atoms to produce NCO.

As reference, the gaseous CO molecule was optimized obtaining a C–O distance of 1.142 Å and for the vibrational frequency a wavenumber of 2140 cm^{-1}. These results are in good agreement with the experimental ones, 1.128 Å and 2145 cm^{-1}, respectively [52]. The gaseous NCO radical was also optimized obtaining N–C and C–O distances of 1.229 Å and 1.195 Å, respectively, and, for the asymmetric and symmetric vibrational frequencies, the values of 1981 cm^{-1} and 1256 cm^{-1}, respectively. These results are in rather good agreement with the experimental ones: 1.20 Å for the N–C distance [53], 1951 cm^{-1} and 1279 cm^{-1} for the asymmetric/symmetric vibrational frequencies [54,55].

Regarding the adsorption of individual N atoms on both (100) and (111) faces of Pd, our calculations support the fact that the most favored sites are the more coordinated ones; i.e., the fourfold for the (100) and the threefold (FCC and HCP) for the (111), respectively. These results are in agreement with previous theoretical and experimental findings [22,26]. Adsorption energies are in the range −5.1 to −4.7 eV.

The calculations corresponding to the CO molecule on Pd(100) support the fact that the most stable sites are the twofold ones, whereas on Pd(111), they are the threefold (FCC and HCP) ones. This is in agreement with other calculations and the experiments for low, medium or high CO coverage on Pd(100) [18,19,56] and for low coverage on Pd(111) [25,57]. Adsorption energies are in the range −1.3 to −1.9 eV, although on the (100) face the calculated adsorption energy values for bridge and hollow sites are close. The obtained C–O and C–Pd distances and asymmetric frequencies for CO are in very good agreement with experiments as can be observed in Table 1.

In the case of the adsorption of NCO species, the hollow sites are the most favored on both (100) and (111) faces of Pd. Adsorption energies are in the range −2.3 to −2.9 eV. Taking into account the (100) face, the calculated adsorption energy values for bridge and hollow sites are very close. Moreover, these results are coincident with those of a previous work for coverage of 1/4ML [33]. The C–O interatomic distance shows a small decrease and the N–C one an increase, compared to the free NCO species (1.195 Å and 1.229 Å, respectively). In addition, we observe a shortening in the C–O distance of adsorbed NCO comparing with that distance in adsorbed CO; such change in the bond distance can be related to the different electronic structure of these molecules (see section 3.2.4). For the asymmetric vibrational frequency of adsorbed NCO, we computed a value of 2195 cm^{-1}, close to 2156 cm^{-1} obtained in a previous theoretical work [33] and to 2134 cm^{-1} reported by Solymosi et al.

Table 1
Adsorption energies E_{ads} (in eV), frequencies υ (in cm^{-1}), and distances d (in Å), for the N, CO and NCO individually adsorbed species on top, bridge and hollow sites, for $\theta = 0.25$. Reference values are between brackets. The "*" symbol indicates the experimental values.

	Pd(100)						
	N_{hollow}	CO_{top}	CO_{bridge}	CO_{hollow}	NCO_{top}	NCO_{bridge}	NCO_{hollow}
E_{ads}	−5.106 (−4.2)[a]	−1.474 (−1.44)[b]	−1.902 (−1.92)[b]	−1.865 (−1.74)[b]	−2.351	−2.918	−2.897
υ		2051 (2062)[b]	1892 (1887)[b] (*1910)[c]	1708 (1828)[b]	2240	2245	2195 (*2134)[c]
$d_{N\text{-}Pd}$	2.024				1.955	2.080	2.302
$d_{C\text{-}O}$		1.157 (1.16)[b]	1.176 (1.17) [b]	1.201 (1.19)[b]	1.206	1.186	1.180
$d_{N\text{-}C}$					1.204	1.222	1.240
$d_{C\text{-}Pd}$		1.878 (1.88)[b]	2.004 (2.01)[b]	2.209 (2.24)[b]			

	Pd(111)						
	N_{FCC}	N_{HCP}	CO_{top}	CO_{bridge}	$CO_{hollow\ FCC/\ HCP}$	$NCO_{hollow\ FCC}$	$NCO_{hollow\ HCP}$
E_{ads}	−4.745 (−4.01)[d]	−4.607 (−3.91)[d]	−1.336 (−1.43)[e]	−1.760 (−1.85)[e]	−1.923 (−2.00)[e]	−2.800	−2.668
υ			2061 (2046)[e]	1886 (1871)[e]	1814 (1802/1779)[e] (*1807)[f]	2230 (*2242)[g]	2231
$d_{N\text{-}Pd}$	1.920	1.918				2.161	2.168
$d_{C\text{-}O}$			1.156 (1.16)[e]	1.178 (1.18)[e]	1.187 (1.19)[e]	1.182	1.182
$d_{N\text{-}C}$						1.229	1.229
$d_{C\text{-}Pd}$			1.874 (1.87)[e]	2.003 (2.00)[e]	2.084 (2.09)[e]		

[a] For $\theta = 0.25$ [23].
[b] For $\theta = 0.5$ [18].
[c] [7,14].
[d] For $\theta = 0.25$ [26].
[e] For $\theta = 0.25$ [25].
[f] [3].
[g] [3] FCC or HCP.

from RAIS spectra for low NCO coverage [14]. With regard to the NCO adsorption on Pd(111), we considered in principle the adsorption on the four possible sites of this surface: top, bridge, FCC hollow and HCP hollow. Absolute minima (without imaginary frequencies) were obtained only for the adsorption on the hollow sites, being the FCC site 0.13 eV more stable than the HCP site. It is worth mentioning that beginning with the NCO species located on a bridge site, it finished on a FCC hollow site. While the interatomic C–O distance is somewhat shorter than that for free NCO and almost equal to that of the adsorbed CO, the N–C distance does not change. Regarding the asymmetric vibrational frequency of adsorbed NCO, our value of 2230 cm^{-1} is in very good agreement to that reported by Goodman et al. [3]. Indeed, a peak at 2242 cm^{-1} which would correspond to an adsorbed NCO species was obtained by these authors [3] from PM-IRAS spectra for the CO + NO reaction over Pd(111) with $P = 2.7 \times 10^{-3}$ mbar and $T = 600$ K. The larger vibrational frequency for the (111) face could be associated with a shorter N–Pd distance and weaker N–C bond, compared to the (100) face. It is to be noticed that no other experimental or theoretical data for the adsorption energy, frequencies and interatomic distances of adsorbed NCO on Pd(111) have been reported in the literature.

3.2. NCO formation

3.2.1. Coadsorbed species

According to the experimental and theoretical information, the CO molecule adsorbs primarily on Pd(100) bridge sites over the entire surface coverage range [56], whereas on Pd(111) it prefers hollow sites at low coverage ($\theta = 0.33$ML) and either bridging or hollow sites at medium coverage ($\theta = 0.50$ML) [57]. On the other hand, compared to CO, our calculations show a larger stability of adsorbed N atom for both studied surfaces with an adsorption energy difference of 3.2 eV in Pd(100) and 2.7 eV in Pd(111) (see Table 1). Hence, we can infer a relative easy diffusion process for the CO molecules on the (100) and (111) faces of palladium, jumping between bridging and/or hollow sites, whereas the N atoms remain fixed on hollow sites. In order to define which initial configuration will be adopted for the reaction between CO and N, different coadsorption possibilities were evaluated. In the case of the (100) surface, the CO molecule was located on a bridge or hollow site and the N atom on a hollow site. After optimization, the results showed that two situations can be selected as initial configurations for the reacting CO and N, with the adsorbed species being second and first neighbors, respectively, on fourfold hollow sites (see Scheme 1a and b). The first geometrical configuration became about 0.60 eV more favorable than the second. With regard to the (111) surface, a similar procedure defines the following two situations: one with the N atom and the CO molecule coadsorbed on two neighboring hollow FCC sites, and the other with the N atom on a hollow FCC site and the CO molecule on a contiguous hollow HCP site (see Scheme 1c and d). The first configuration is ~0.10 eV more favorable than the second. On the other hand, from the E_{ads} values of Table 1, we note that the NCO species could be adsorbed

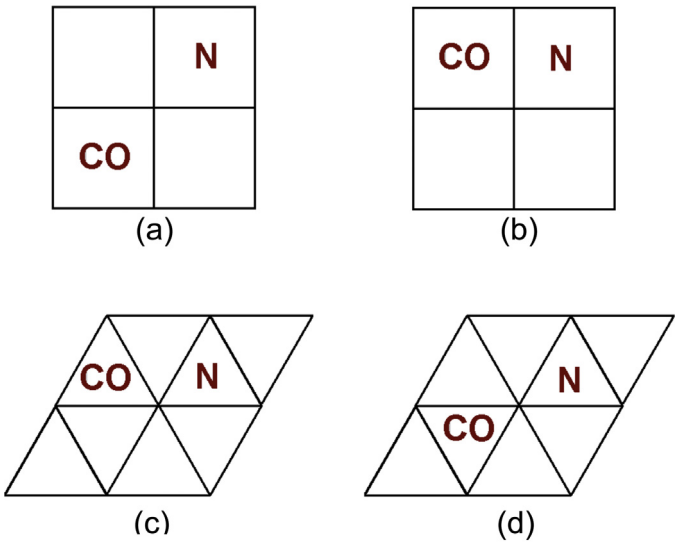

Scheme 1. Initial configuration adopted for the N + CO surface reaction. On Pd(100), with the adsorbed species as second (a) or first (b) neighbors; on Pd(111), with both adsorbed species in hollow FCC sites (c), or with the N atom in a hollow FCC site and the CO molecule in a contiguous hollow HCP site (d).

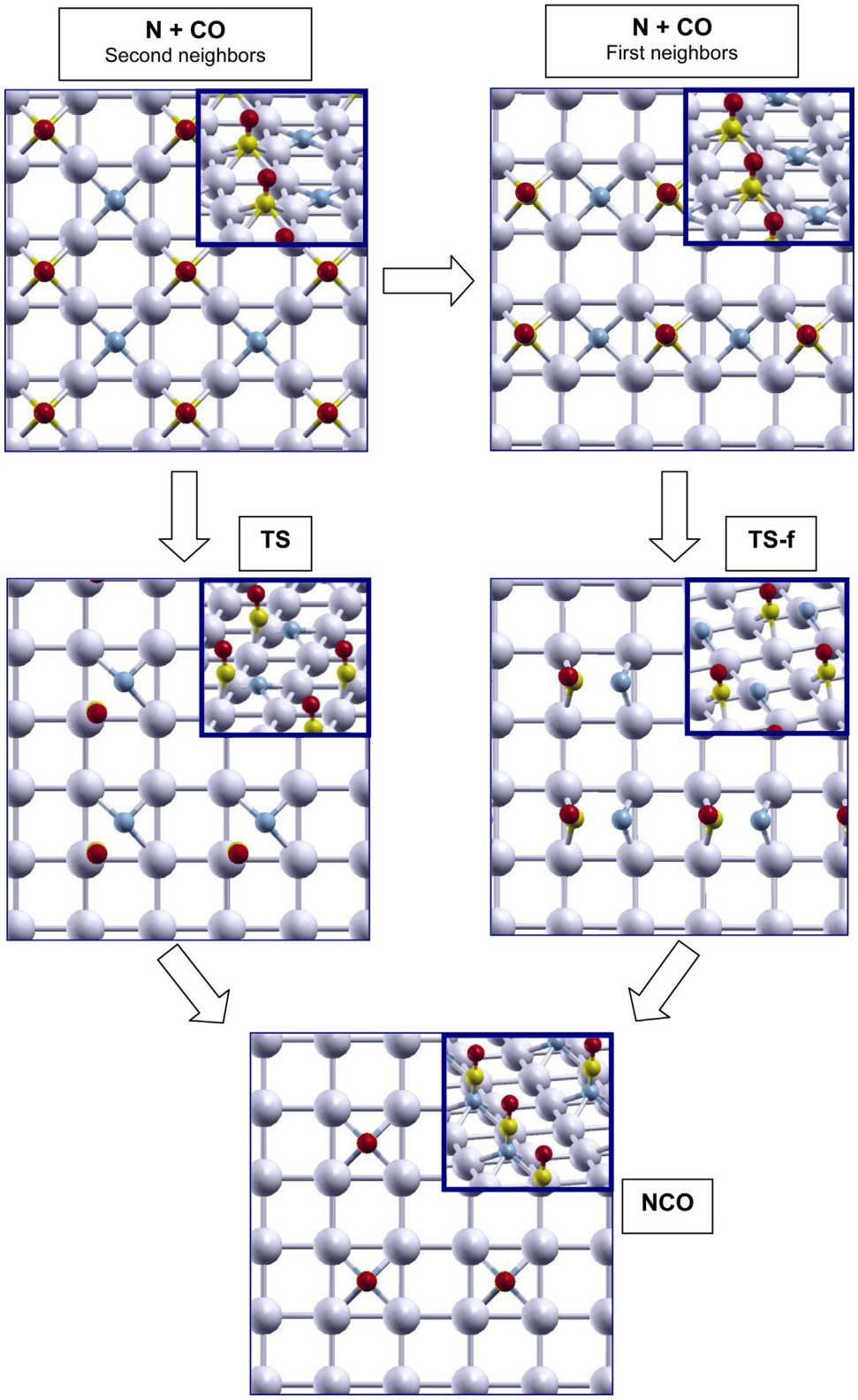

Fig. 1. Top and perspective views of the geometry of CO and N species in the NCO formation on Pd(100) according to the "top" (left) and the "bridge-bridge" (right) pathways, passing through TS and TS-f transition states, respectively. The spheres represent: first layer Pd atoms (gray), N atoms (light blue), C atoms (yellow) and O atoms (red). (For interpretation of the references to color in this figure legend, the reader is referred to the web version of the article.)

on a bridging or a hollow site on Pd(100) (these geometries differ by only 0.02 eV), or on a hollow FCC on Pd(111). Hence, for both Pd surfaces, after the insertion of CO to N to yield the NCO species, the product will be on a high coordination site.

3.2.2. The reaction on Pd(100)

Two different pathways were proposed for the $N + CO \rightarrow NCO$ reaction shown in Fig. 1, taking into account the possible initial geometries for coadsorbed N and CO and for the final produced

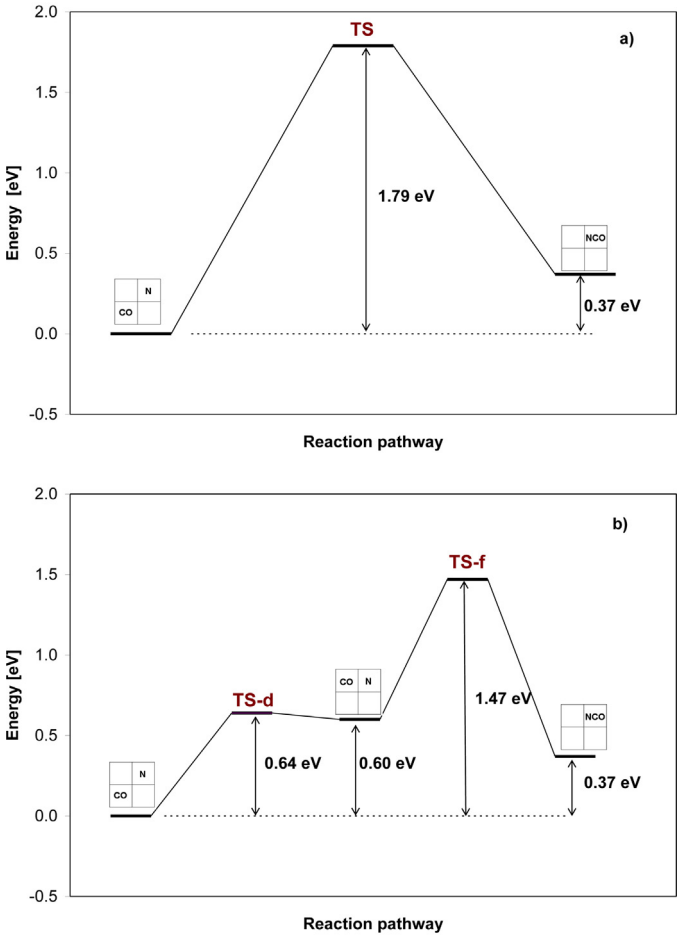

Fig. 2. Energy profile for the NCO formation on Pd(100), corresponding to: (a) the "top" reaction pathway and (b) the "bridge-bridge" reaction pathway (see Fig. 1).

NCO as outlined in precedent paragraph. In the first one, the CO and N species begin separated and adsorbed at second neighboring hollow sites (see Scheme 1a), then the CO molecule crosses upon a top site, defining a transition state TS, and finishes linked to the N atom forming NCO on the corresponding hollow site. This mechanism has been designed like the "top" pathway. In the second one, the CO and N species begin having the same initial locations; afterwards the CO molecule migrates to a first neighboring hollow site (see Scheme 1b), defining a diffusion transition state TS-d, crosses over another bridge site with a transition state TS-f and finally combines with the N atom. This mechanism has been designed like the "bridge-bridge" pathway. In Fig. 2, the energies of different steps of these mechanisms are reported, taking as zero reference the initial geometrical configuration. Notice that the reaction in this case corresponds to an endothermic process that requires 0.37 eV. The overall energetic barriers are in the range 1.5–1.8 eV, being the largest that for the "top" pathway. The diffusional barrier of the first step of "bridge-bridge" pathway has an energetic cost of 0.64 eV and the subsequent barrier through the TS-f state has a requirement of 0.87 eV, much lower than that through the TS state (1.79 eV). It was observed that for the TS as well as for the TS-f states the N–C bond is about 1.9–2.0 Å long, shortening significantly (~0.7 Å shorter) only when the adsorbed NCO is just formed (see Table 1).

3.2.3. The reaction on Pd(111)

In the same way as for the (100) face of Pd, and considering the possible initial geometries for coadsorbed N and CO and that for the NCO species, two different pathways were proposed for the N + CO → NCO reaction on the (111) face (Fig. 3). In the first one, the CO and N species are initially separated and adsorbed at first neighboring hollow FCC sites (see Scheme 1c), then the CO molecule crosses over two bridge sites that are close to a lateral top site, defining a transition state TS, and finishes linking with the N atom. This mechanism has been designed like the "double bridge" pathway. In the second mechanism, the CO and N species are initially in the same locations as in the first one, afterwards the CO molecule migrates to an adjacent hollow HCP site (see Scheme 1d), defining a diffusion transition state TS-d, crosses over a top site with a transition state TS-f and finishes combining with the N atom. This mechanism has been designed like the "bridge-top" pathway. In Fig. 4, the energies of different steps of these mechanisms are reported, taking as zero reference the initial geometrical configuration. The reaction on this surface corresponds to an exothermic process that liberates 0.50 eV. The overall energetic barriers are of nearly 1.1 eV, in both cases studied. The diffusional barrier of the first step of "bridge-top" pathway has an energetic cost of 0.25 eV and the subsequent barrier through the TS-f state has an energy requirement that is only 0.12 eV lower than that through the TS state (1.10 eV).

3.2.4. Analysis of the N + CO → NCO reaction

From the results of previous sections, we can infer that the formation of NCO radical from N and CO is a more favored process on the (111) face of palladium than on the (100) face owing to two confluent factors: an exothermicity versus endothermicity behavior and a lower activation barrier. Moreover, this is evident in the two reaction pathways studied on palladium surfaces: the direct and the indirect one, which requires a diffusion step. In the present section we will consider how the electronic structure governs these properties.

In Tables 2 and 3, the atomic net charges obtained using the Voronoi analysis are summarized at the initial, the highest transition state and the final position along the two reaction pathways above considered. In these Tables the charges of CO and NCO as fragments are also detailed. Notice firstly that on both surfaces all the adsorbed species are negatively charged and, correspondingly, a polarization of nearer Pd atoms acquiring in mean a compensatory positive charge is present. Moreover, notice that the reactants have larger negative charges on the (100) than on the (111) face and that, on the other hand, on the latter surface the N and CO fragments of the final product have more negative and more positive charges, respectively. Besides, on both surfaces and as a consequence of the combination of N and CO, a large electronic charge is transferred from the NCO, as an entity, towards the Pd substrate. In order to gain more insight on the role played by this charge redistribution, in Table 4 are summarized the electronic charge variations calculated with respect to the initial state of the reaction. The charge lost by NCO as an entity, Δq, is closely equal to that gained by the Pd atoms of the first layer ($\Delta q \sim 1.13$ e on Pd(100) and $\Delta q \sim 0.82$ e on Pd(111), see Table 4). The C atom is the species more affected in the lost of charge ($\Delta q \sim 0.70$ e in Pd(100) and $\Delta q \sim 1.03$ e in Pd(111)), compared with that of N and the O atoms ($\Delta q \sim 0.33/0.03$ e and $\Delta q \sim 0.10/-0.24$ e, respectively). This shows that the NCO radical has become a more polarized species on Pd(111) than on Pd(100) and that, therefore, a larger stabilization should be expected in the former case. Regarding the transition states for the two faces, it is interesting to note that although we cannot appreciate a large difference in the charge acquired by the palladium atoms (between 0.4 e and 0.5 e), when we go from the initial position to the highest transition states, the major values (0.5 e) correspond to the cases where the CO molecule crosses over a top site (that is, TS for the (100) face and TS-f for the (111) face). It is also a remarkable fact that the C–O bond becomes shorted to ~1.16 Å when this molecule achieves any of these transition states, an observation that is in agreement to the

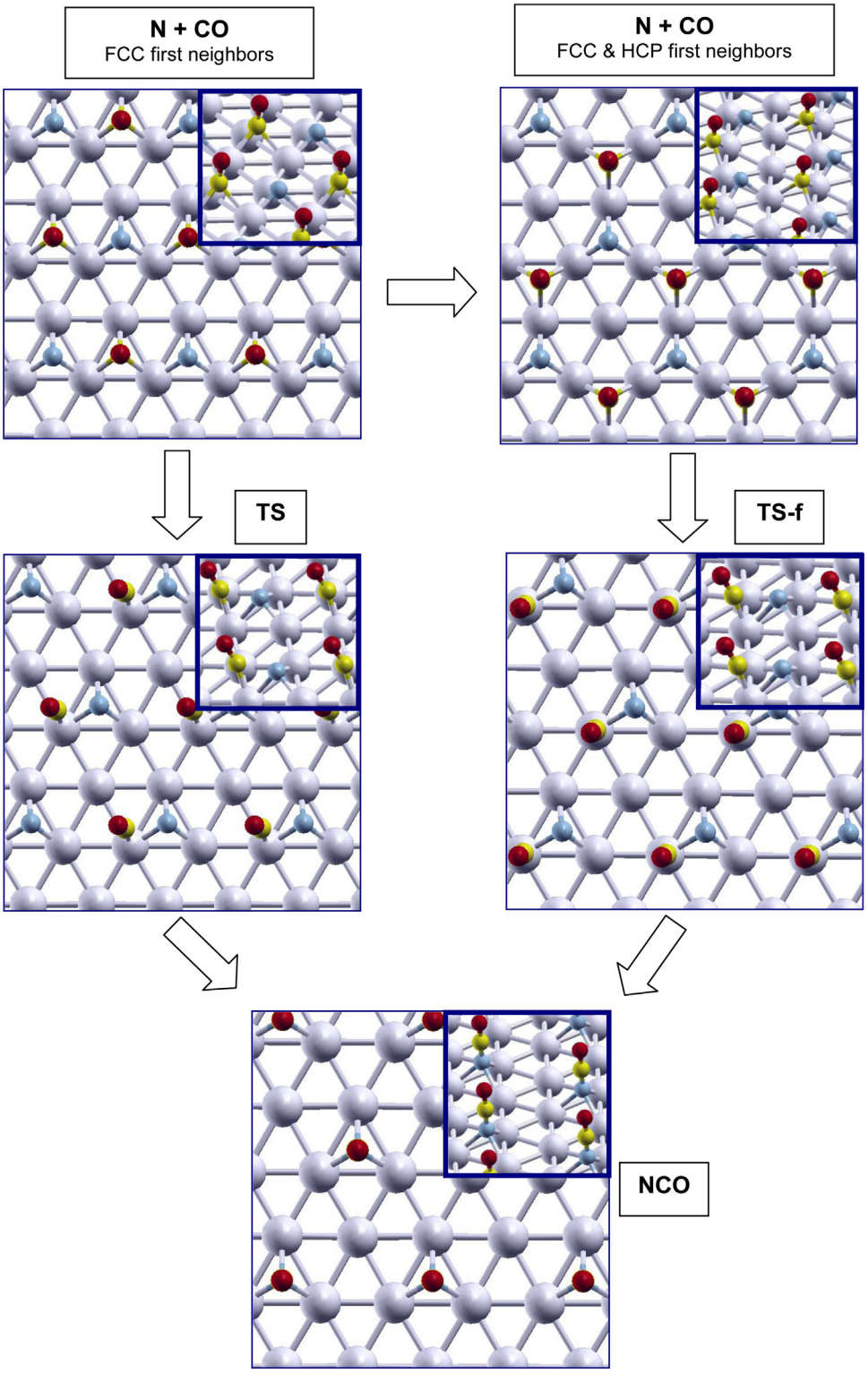

Fig. 3. Top and perspective view of the geometry of CO and N species in the NCO formation on Pd(111) according to the "double bridge" (left) and the "bridge-top" (right) pathways, passing through TS and TS-f transition states, respectively. The spheres represent: first layer Pd atoms (gray), N atoms (light blue), C atoms (yellow) and O atoms (red). (For interpretation of the references to color in this figure legend, the reader is referred to the web version of the article.)

strengthening of C–O bond due to the lost of electronic charge of CO fragment and the contingent population decrease of its antibonding $2\pi^*$ orbitals.

In order to analyze the electronic structure corresponding to the highest transition states, the LDOS for the TS of "top" and the TS-f of "bridge-top" pathways for the (100) and (111) faces of Pd were calculated, respectively. These states were selected because they show analogous geometrical symmetry; i.e., the CO molecule crosses in both cases over a top site, the differences coming eventually from the bonding between the transition state and the different faces of Pd. In Fig. 5a and b, we show the LDOS of the p_x, p_y and p_z orbitals of C and N atoms, respectively, and simultaneously the

Table 2
Voronoi net charge (in e) of N, C, O atoms, CO and NCO species and palladium atoms of first layer (Σ Pd's) for the reaction pathways on Pd(100).

	Pd(100)					
	N	C	O	CO	NCO	Σ Pd's
N + CO	−1.140	−0.377	−0.334	−0.711	−1.851	+1.676
TS (top)	−0.951	−0.050	−0.193	−0.243	−1.194	+1.162
TS-f (bridge-bridge)	−0.814	−0.146	−0.275	−0.421	−1.235	+1.266
NCO	−0.809	+0.326	−0.235	+0.091	−0.718	+0.642

Table 3
Voronoi net charge (in e) of N, C, O atoms, CO and NCO species and palladium atoms of first layer (Σ Pd's) for the reaction pathways on Pd(111).

	Pd(111)					
	N	C	O	CO	NCO	Σ Pd's
N + CO	−0.984	−0.380	−0.151	−0.531	−1.515	+1.575
TS (double bridge)	−0.934	+0.038	−0.214	−0.176	−1.110	+1.144
TS-f (bridge-top)	−0.854	+0.041	−0.211	−0.170	−1.024	+1.061
NCO	−0.957	+0.654	−0.389	+0.265	−0.692	+0.653

Table 4
Changes of Voronoi net charges (Δq) of N, C, O, NCO and palladium atoms of first layer (Σ Pd's), going from the initial state with separated species to the higher energy transition states or the final formed NCO. The "+" symbol indicates a lost of electrons.

	Pd(100)					Pd(111)				
	Δq N	Δq C	Δq O	Δq NCO	Δq Σ Pd's	Δq N	Δq C	Δq O	Δq NCO	Δq Σ Pd's
to TS	+0.189	+0.327	+0.141	+0.657	−0.514	+0.050	+0.418	−0.063	+0.405	−0.431
to TS-f	+0.326	+0.231	+0.059	+0.616	−0.410	+0.130	+0.421	−0.060	+0.491	−0.514
to NCO	+0.331	+0.703	+0.099	+1.133	−1.034	+0.027	+1.034	−0.238	+0.823	−0.922

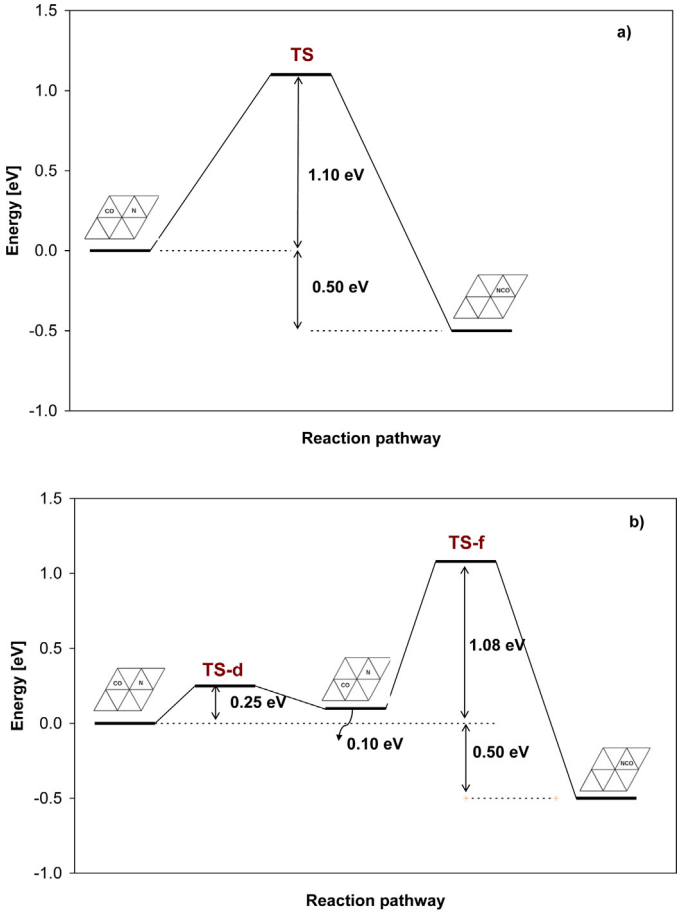

Fig. 4. Energy profile for the NCO formation on Pd(111) corresponding to: (a) the "double bridge" reaction pathway and (b) the "bridge-top" reaction pathway (see Fig. 3).

LDOS of d-orbitals of the nearest Pd atom for the TS of "top" pathway (Pd(100) surface). In both cases, the Pd d-band expands up to 6 eV below the Fermi level and it presents a narrow peak located at about −6.5 eV. With respect to the LDOS of N the more important contribution comes from states between 5 and 6 eV below of Fermi level, in the lower region of the Pd d-band, whereas that corresponding to the LDOS of C atom is localized mainly around the level at ∼−6.5 eV. Moreover, the N levels show a non negligible coupling with the Pd-d states along all the d-band, in contrast to the case of C levels. A similar inference can be obtained from the LDOS curves corresponding to the TS-f of "bridge-top" pathway (Pd(111) surface). For this reason we can think that the role of N orbitals is more significant than those of the C atom in the bonding between Pd and NCO.

Fig. 6a and b shows the LDOS for the p_x, p_y and p_z orbitals of N atoms, and the LDOS of Pd d-orbitals for the TS and TS-f states on Pd(111) and Pd(100), respectively. Notice that the Pd d-states located above the bottom of Pd d-band are the most involved in coupling with the N p-states. Hence, the degree of coincidence observed between the electronic states of adsorbed species and those of the metal can be related to the magnitude of the corresponding activation barrier at the transition state. A larger coincidence means a stronger interaction and a lower activation barrier. Then, provided that in the transition states for the studied "top" and "bridge–top" pathways (for Pd(100) and Pd(111), respectively), the adsorbed species adopts a similar geometry (see Figs. 1 and 3), it is possible to appeal to such coincidence in order to predict the relative magnitude of the corresponding activation barriers (see Figs. 2a and 4b). A way to quantify this effect is through the following K parameter:

$$K = 1 - \left[\frac{\left| \int \mathrm{LDOS(N\ p\text{-}orbitals)}\, d\varepsilon - \int \mathrm{LDOS(Pd\ d\text{-}orbitals)}\, d\varepsilon \right|}{\int \mathrm{LDOS(N\ p\text{-}orbitals)}\, d\varepsilon} \right] \quad (4)$$

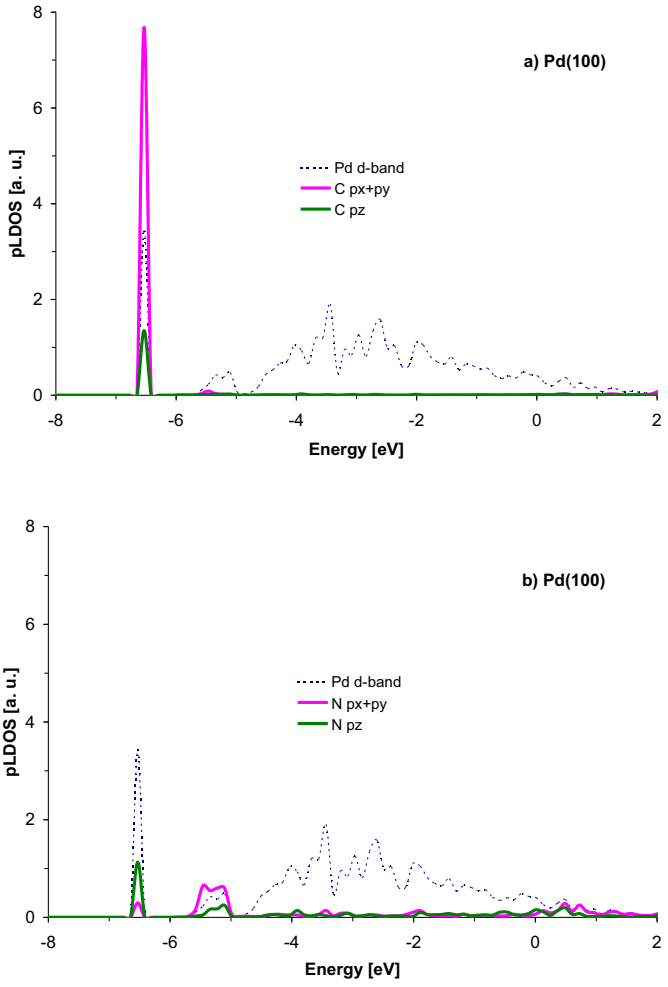

Fig. 5. Partial local density of states (pLDOS) corresponding to the NCO formation on Pd(100), at the transition state for the "top" pathway. The carbon p-orbitals (a), nitrogen p-orbitals (b) and palladium d-band contributions from spin up states are represented. The zero on the energy axis corresponds to the Fermi level.

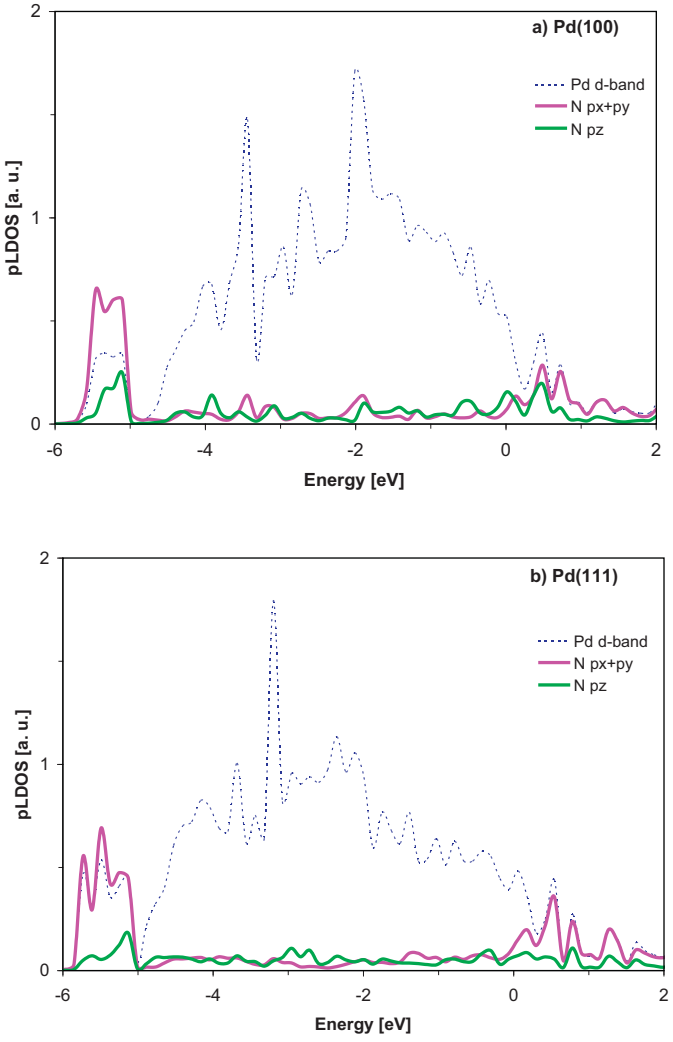

Fig. 6. Partial local density of states (pLDOS) for the NCO formation on palladium surfaces, at the transition states for: (a) the "top" pathway on Pd(100) and (b) the "double bridge" pathway on Pd(111). The nitrogen p-orbitals and palladium d-band contributions from spin up states are represented. The zero on the energy axis corresponds to the Fermi level.

where $\int \mathrm{LDOS(N\,p\text{-}orbitals)}\,d\varepsilon$ is the contribution of p_x, p_y, p_z orbitals of N atom to states in the −5 eV to −6 eV range of energies and $\int \mathrm{LDOS(Pd\,d\text{-}orbitals)}\,d\varepsilon$ is the contribution of d-orbitals of the nearest Pd atom in the same range of energies. In this way, when $K \cong 1$ the coincidence is larger in the given energy interval. The results have been summarized in Table 5. Notice that the value of the K parameter for the (111) face is larger than that for the (100) face. This result is compatible with the presence of a relatively lower activation barrier in the case of Pd(111) (1.08 eV vs. 1.79 eV).

Table 5
Integrated areas (in a.u.) calculated from pLDOS curves (Fig. 6a and b) and correlation parameter K (see section 3.2.4) for the transition state barriers of the "top" and "bridge-top" reaction pathways on Pd(100) and Pd(111), respectively.

		Pd(100)	Pd(111)
Orbitals	Pd-*d*	1.51	2.64
	N-p_x,p_y	2.70	2.94
	N-p_z	0.70	0.57
K		0.44	0.75
Energy Barrier (eV)		1.79	1.08

4. Conclusions

The theoretical approach accomplished in this work to study the N + CO → NCO reaction on the Pd(100) and Pd(111) surfaces allow us to arrive to the following conclusions:

(1) The coadsorbed N and CO species prefer to be adsorbed on highly coordinated sites of these two surfaces before to combine. Two different pathways were considered on both surfaces. They comprise the displacement of CO species between two contiguous hollow sites or an intermediate diffusion step over bridge sites.
(2) The thermodynamic balance shows that for a coverage of 1/4ML the reaction is endothermic on Pd(100) and exothermic on Pd(111). The endo-versus exothermicity can be explained taking into account the larger NCO electronic polarization on Pd(111).
(3) The resulting energy barriers are larger on Pd(100), compared with Pd(111). The presence of smaller energy barriers for Pd(111) can be related to a larger coupling of p-orbitals of N with d-orbitals of Pd.

(4) The production of NCO is largely favored on Pd(111) in comparison with Pd(100).This consequence is in complete agreement with the experimental findings of Goodman et al.
(5) The theoretical vibrational frequencies obtained for NCO adsorbed on highly coordinated sites of Pd(100) and Pd(111) are in good agreement with previously reported IR data.

Acknowledgements

The authors want to acknowledge the financial support of these Argentine institutions: Consejo Nacional de Investigaciones Científicas y Técnicas, Agencia Nacional de Promoción Científica y Tecnológica and Universidad Nacional del Sur, under Grants PIP No. 112-200801-02286, PICT-2010-0830 and PGI 24/F05, respectively.

References

[1] B. Hammer, J. Catal. 199 (2001) 171–176.
[2] K. Honkala, P. Pirilä, K. Laasonen, Surf. Sci. 489 (2001) 72–82.
[3] E. Ozensoy, D.W. Goodman, Phys. Chem. Chem. Phys. 6 (2004) 3765–3778.
[4] L. Piccolo, C.R. Henry, J. Mol. Catal. A: Chem. 167 (2001) 181–190.
[5] C. Neyertz, M. Volpe, D. Pérez, I. Costilla, M. Sánchez, C. Gígola, Appl. Catal. A 368 (2009) 146–157.
[6] F. Gao, Y. Wang, D.W. Goodman, J. Catal. 268 (2009) 115–121.
[7] X. Xu, P. Chen, D.W. Goodman, J. Phys. Chem. 98 (1994) 9242–9246.
[8] D.R. Rainer, S.M. Vesecky, M. Koranne, W.S. Oh, D.W. Goodman, J. Catal. 167 (1997) 234–241.
[9] G.R. Garda, R.M. Ferullo, N.J. Castellani, Surf. Rev. Lett. 8 (2001) 641–651.
[10] M.L. Unland, J. Catal. 31 (1973) 459–465.
[11] D.C. Chambers, D.E. Angove, N.W. Cant, J. Catal. 204 (2001) 11–22.
[12] C. Hess, E. Ozensoy, D.W. Goodman, J. Phys. Chem. B 107 (2003) 2759–2764.
[13] E. Ozensoy, C. Hess, D.W. Goodman, J. Am. Chem. Soc. 124 (2002) 8524–8525.
[14] R. Németh, J. Kiss, F. Solymosi, J. Phys. Chem. C 111 (2007) 1424–1427.
[15] J.E. Jones, M. Trenary, J. Phys. Chem. C 112 (2008) 20443–20450.
[16] H. Celio, K. Mudalige, P. Mills, M. Trenary, Surf. Sci. 394 (1997) L168–L173.
[17] K. Honkala, P. Pirilä, K. Laasonen, Phys. Rev. Lett. 86 (2001) 5942–5945.
[18] A. Eichler, J. Hafner, Phys. Rev. B 57 (1998) 10110–10114.
[19] F. Delbecq, P. Sautet, Phys. Rev. B 59 (1999) 5142–5153.
[20] D. Loffreda, D. Simon, P. Sautet, Chem. Phys. Lett. 291 (1998) 15–23.
[21] D. Loffreda, D. Simon, P. Sautet, Surf. Sci. 425 (1999) 68–80.
[22] F. Delbecq, P. Sautet, Surf. Sci. 442 (1999) 338–348.
[23] D. Loffreda, D. Simon, P. Sautet, J. Chem. Phys. 108 (1998) 6447–6457.
[24] M.W. Wu, H. Metiu, J. Chem. Phys. 113 (2000) 1177–1183.
[25] C. Fan, W.-D. Xiao, Comput. Theor. Chem. 1004 (2013) 22–30.
[26] J.A. Herron, S. Tonelli, M. Mavrikakis, Surf. Sci. 606 (2012) 1670–1679.
[27] S. Zhao, Y.-L. Ren, J.-J. Wang, W.-P. Yin, J. Mol. Struct. Theochem. 897 (2009) 100–105.
[28] S. Zhao, Y-L. Ren, J-J. Wang, W-P. Yin, J. Phys. Chem. A 113 (2009) 1075–1085.
[29] H. Yang, J.L. Whitten, Surf. Sci. 401 (1998) 312–321.
[30] J.M. Hu, Y. Li, J.Q. Li, Y.F. Zhang, W. Lin, G.X. Jia, J. Solid State Chem. 177 (2004) 2763–2771.
[31] G.R. Garda, R.M. Ferullo, N.J. Castellani, Surf. Sci. 598 (2005) 57–67.
[32] P.G. Belelli, G.R. Garda, R.M. Ferullo, Surf. Sci. 605 (2011) 1202–1208.
[33] P.G. Belelli, M.M. Branda, G.R. Garda, R.M. Ferullo, N.J. Castellani, Surf. Sci. 604 (2010) 442–450.
[34] B.-Z. Sun, W.-K. Chen, Y.-J. Xu, J. Chem. Phys. 131 (2009) 174503–174508.
[35] X. Xu, J. Szanyi, Q. Xu, D.W. Goodman, Catal. Today 21 (1994) 57–69.
[36] D.R. Rainer, M.C. Wu, D.I. Mahon, D.W. Goodman, J. Vac. Sci. Technol. A 14 (1996) 1184–1188.
[37] C.R. Henry, C. Chapon, C. Duriez, S. Giorgio, Surf. Sci. 253 (1991) 177–189.
[38] S. Giorgio, C.R. Henry, C. Chapon, J.M. Penisson, J. Cryst. Growth 100 (1990) 254–260.
[39] G. Kresse, J. Hafner, Phys. Rev. B 47 (1993) 558–561.
[40] G. Kresse, J. Hafner, Phys. Rev. B 48 (1993) 13115–13118.
[41] G. Kresse, J. Hafner, Phys. Rev. B 49 (1994) 14251–14268.
[42] P. Blochl, Phys. Rev. B 50 (1994) 17953–17978.
[43] G. Kresse, D. Joubert, Phys. Rev. B 59 (1999) 1758–1775.
[44] J.P. Perdew, J.A. Chevary, S.H. Vosko, K.A. Jackson, M.R. Pederson, D.J. Singh, C. Fiolhais, Phys. Rev. B 46 (1992) 6671–6687.
[45] J.P. Perdew, J.A. Chevary, S.H. Vosko, K.A. Jackson, M.R. Pederson, D.J. Singh, C. Fiolhais, Phys. Rev. B 48 (1993) 4978.
[46] H.J. Monkhorst, J.D. Pack, Phys. Rev. B 13 (1976) 5188–5192.
[47] M. Methfessel, A.T. Paxton, Phys. Rev. B 40 (1989) 3616–3621.
[48] H. Jónsson, G. Mills, K.W. Jacobsen, Classical and Quantum Dynamics in Condensed Phase Simulations, World Scientific, Singapore, 1998.
[49] G. Mills, H. Jónsson, Phys. Rev. Lett. 72 (1994) 1124–1127.
[50] G. Mills, H. Jónsson, G. Schenter, Surf. Sci. 324 (1995) 305–337.
[51] A.D. Becke, R.M. Dickson, J. Chem. Phys. 89 (1988) 2993–2997.
[52] M. Gajdos, A. Eicherler, J. Hafner, J. Phys. Condens. Matter 16 (2004) 1141–1164.
[53] P. Misra, C.W. Mathews, D.A. Ramsay, J. Molec. Spectrosc. 130 (1988) 419–423.
[54] M. Grubele, M. Polak, R.J. Saykally, J. Chem. Phys. 86 (1987) 6631–6636.
[55] J. Werner, W. Seebass, K. Koch, R.F. Curl, W. Urban, J.M. Brown, Mol. Phys. 56 (1985) 453–461.
[56] J. Szanyi, W.K. Kuhn, D.W. Goodman, J. Vac. Sci. Technol. A 11 (1993) 1969–1974.
[57] M.K. Rose, T. Mitsui, J. Dunphy, A. Borg, D.F. Ogletree, M. Salmeron, P. Sautet, Surf. Sci. 512 (2002) 48–60.